Geophysical Research Letters®

Key Points:

- Seasonal stratification in shelf seas is expected to increase under global heating
- The increase in thermal expansivity with temperature increases the buoyancy forcing that drives seasonal stratification
- The close balance between buoyancy input and mixing amplifies this effect leading to large relative changes in stratification

Why Is Seasonal Density Stratification in Shelf Seas Expected to Increase Under Future Climate Change?

Jason Holt[1] , **James Harle[2]**, **Sarah Wakelin[1]** , **Jenny Jardine[1]** , and **Joanne Hopkins[1]**

[1]National Oceanography Centre, Liverpool, UK, [2]National Oceanography Centre, Southampton, UK

Abstract Coastal and shelf seas provide a diverse range of ecosystem services, which are often mediated by seasonal density stratification through its control on biogeochemical cycles. These seas are highly vulnerable to climate change and downscaling studies consistently project an increase in seasonal stratification over the next century, but without a clear explanation. Here we revisit a well-established theory of coastal ocean mixing and demonstrate with a new ensemble of downscaled simulations for the Northwest European continental shelf seas to 2100 that the increase of expansivity with temperature is sufficient to consistently increase the seasonal stratification. Where there is a closed balance between buoyancy input and mixing, small changes in expansivity are amplified to a large relative change in stratification. This simple link between global heating and stratification substantially reduces uncertainty in projections of this key parameter in seas around the world.

Plain Language Summary Coastal and shelf seas provide a diverse range of benefits to society such as food from fisheries and drawdown of atmospheric carbon dioxide. These benefits are often controlled by seasonal cycles of density layering or stratification, which controls how the water column is mixed and how plankton is able to grow. These seas are highly vulnerable to climate change and modeling studies consistently show an increase in seasonal stratification over the next century, but without a clear explanation. Here we revisit a well-established theory of coastal ocean mixing and demonstrate with a new set of model simulations for Northwest European continental shelf seas to 2100 that the increase of how sea water expands with temperature is sufficient to consistently increase the seasonal stratification. In these seas there is a closed balance between surface heating and mixing to control how stratification develops, so small changes in this expansivity are amplified to give a large change in stratification. This simple link between global heating and stratification substantially reduces uncertainty in projections of this key parameter in seas around the world.

1. Introduction

Seasonal density stratification is a ubiquitous feature of the world's oceans that plays a central role in controlling its biogeochemical cycles. It limits the vertical flux of nutrients to the euphotic layer and oxygen to the benthos, and traps dissolved inorganic carbon in deeper waters. Particularly, in the context of seasonally stratified shelf seas, its onset (breakdown) triggers spring (autumn) phytoplankton blooms (Ruiz-Castillo et al., 2019; Wihsgott et al., 2019) and during the summer supports a productive sub-surface chlorophyll maximum (Fernand et al., 2013; Hickman et al., 2012). Where the continental slope generates an internal tide, the strength and structure of summer stratification controls the generation, dissipation and propagation of internal wave energy, with implications for vertical biogeochemical fluxes between surface and bottom waters. Oxygen deficiency is of increasing concern with respect to maintaining healthy and productive seas (Breitburg et al., 2018), and for near-bed oxygen concentrations the balance of stratification and mixing on seasonal time scales is a key controlling process (Queste et al., 2016; Topcu & Brockmann, 2015). Shelf seas contribute a significant but highly uncertain component of the global marine biological carbon pump and cross-pycnocline mixing is an important control on this (Legge et al., 2020; Rippeth et al., 2014).

Seasonal stratification is controlled by cyclic variations in the balance between surface buoyancy forcing and mixing, primarily from wind and tides (Simpson & Bowers, 1981). It is important to distinguish here between seasonal and permanent stratification, particularly in the case of seas that periodically mix to the seabed, and so lack permanent stratification at all. An increase in air temperature necessarily increases permanent stratification until the atmosphere and ocean reach a (dynamic) thermal equilibrium, which can take many decades to centuries for the case of deep ocean or regional sea basins. Seasonal stratification on the other hand resets each annual mixing cycle, allowing equilibrium with the atmosphere to be reached much faster, and so how it

responds to climate change is more nuanced (Holt et al., 2016). For example, the typical timescale of sensible heat-flux adjustment in a 60 m deep well-mixed water column is $C_p \rho h/S \sim 150$ days; that is, much faster than climatic timescales. Here $h = 60$ m is typical water depth, S is a transfer coefficient calculated by the CORE bulk formulas (Large & Yeager, 2004) assuming a 10 m s^{-1} wind speed; C_p is the specific heat capacity and ρ is the water density.

Global Climate Models (GCMs) provide the primary source of information on global scale climate change, delivering simulations to the Coupled Model Intercomparison Project (CMIP) and informing the Intergovernmental Panel on Climate Change assessment reports. However, GCMs generally lack the resolution or process representation to provide reliable simulations in the coastal ocean (Holt et al., 2017). Hence, to develop understanding of coastal ocean response to climate change and provide useful future projections, recourse is often made to dynamical downscaling. This draws on the substantial activity in regional ocean modeling for research and operational oceanography, taking well established regional model configurations and driving them with output from GCMs (see Drenkard et al., 2021 for a discussion on the various approaches). These simulations provide representations of the evolving state of the coastal ocean under various climate change scenarios, acknowledging that errors and biases in the driving information will propagate into the downscaled simulations. Systematic treatment of uncertainty in this context is very challenging since, in addition to emission scenario uncertainty and that associated with the driving climate models, there are layers of uncertainty associated with both the downscaled model itself (structure and parameter choices) and how the GCM forcing is implemented. Hence, even multi-scenario ensembles (as considered here and e.g., (Tinker et al., 2016)) are more useful for understanding process response to change than detailed probabilistic projections; that is, asking what are the range of possible futures and the direction of change? but stopping short of assigning even semi-quantitative likelihood values.

Previous downscaling simulations show a general tendency for seasonal stratification to increase under future climate change forcing, but without much in the way of dynamic analysis. We reviewed 45 published future climate downscaling studies in regional seas around the world (listed in Table S1 in Supporting Information S1). Of these, 37 report a consistent increase in future stratification, 4 report no change or a change dependent on ensemble member, and 4 a decrease. In the 20 cases in tidally active and seasonally stratified seas these are: 16, 2, 2, respectively. This brief survey includes a diverse range of different regional sea types, including both temperature and salinity stratified cases; nonetheless there is a clear pattern of increasing stratification. While air temperature warming is consistent across GCMs (geographically and between ensembles members), other factors driving surface buoyancy flux, such as solar radiation and wind speed are more nuanced. Given the complexity of seasonal stratification in strongly mixed seas, this consistency of increasing stratification is surprising.

In this paper we present a new ensemble of future climate projections for the NW European continental shelf seas and explore how the seasonal stratification changes in these simulations. The energetic theory of seasonal stratification based on the potential energy anomaly (PEA; see Section 2) in shelf seas is well established (Burchard & Hofmeister, 2008; Simpson & Bowers, 1981), but has yet to be exploited as a diagnostic tool for future climate change. Here we use it to draw some straightforward conclusions on the potential future change of seasonal stratification in this context.

2. Methods

2.1. The AMM7 Configuration

For this work we use the Atlantic Margin Model at 7 km (AMM7; Figure 1) configuration of the Nucleus of a European Model of the Ocean; a detailed description is given by (O'Dea et al., 2017). This model has an equal-angle quadrilateral C-grid mesh of 1/15° latitude (7.4 km) by 1/9° longitude (5.2–9.4 km). The vertical discretization uses 51 terrain following levels, compressed toward the surface, and the envelope approach to avoid bathymetric smoothing over steep topography. A k-ε model (Luneva et al., 2019; Umlauf & Burchard, 2003) is used for vertical mixing.

2.2. The Downscaled Ensemble

Surface and lateral boundary conditions, and initial temperature and salinity are taken from 11 CMIP5 (Taylor et al., 2012) GCMs (GFDL-ESM2G, GFDL-ESM2M, HadGEM2-CC, HadGEM2-ES, IPSL-CM5A-LR,
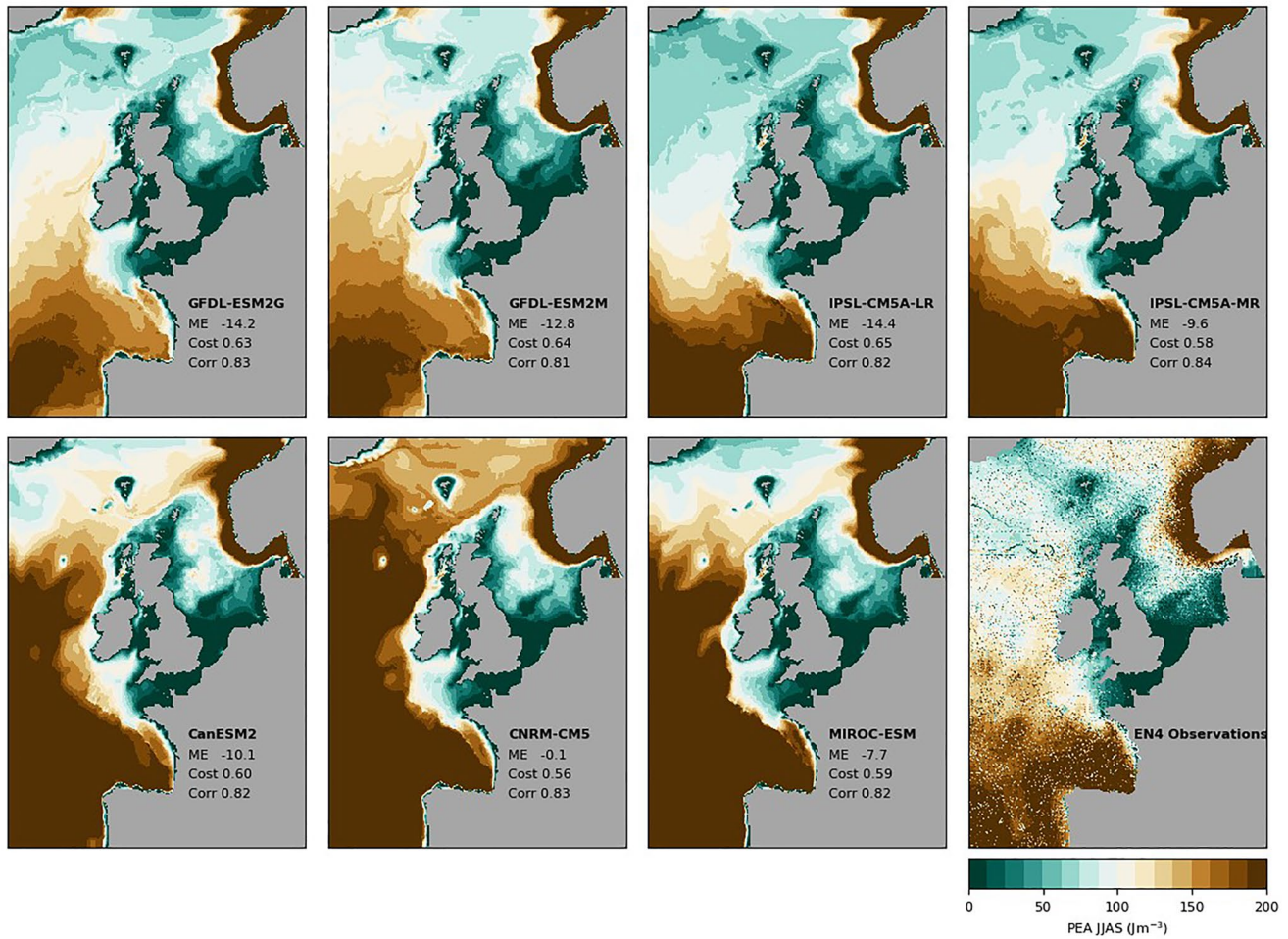
Figure 1. Mean summer stratification (JJAS; potential energy anomaly J m^{-3}) for core ensemble members for the present-day period (1983–2012). Also shown are observations from the EN4 data set (1970–2018). Summer on-shelf error statistics (mean error [J m^{-3}], cost function and correlation) are given for each member; see Table S3 in Supporting Information S1 for details.

IPSL-CM5A-MR, IPSL-CM5B-LR, BCC-CSM1-1-m, CanESM2, CNRM-CM5, and MIROC-ESM; see Table S2 in Supporting Information S1), using daily atmospheric and monthly ocean data following the forcing approach described in (O'Dea et al., 2017). These are used without adjustment or bias correction, apart from at the Baltic open boundary, and were chosen on the basis of data availability to force AMM7 coupled to a biogeochemical model. River forcing is from observed mean annual cycles from 250 rivers at daily frequency (Vörösmarty et al., 2000; Young & Holt, 2007), modulated by the fractional change (compared to 1984–2004 mean) in annual GCM precipitation aggregated over four land regions (1. UK and Ireland; 2. Sweden and Norway; and Continental Europe: 3. east of 2.5°E and 4. west of 2.5°E).

The open boundary connecting the North and Baltic Seas requires special treatment owing to the inadequate representation of the Baltic in most of these CMIP models. Following (O'Dea et al., 2017) we use a present day (2001–2012) climatology from a North Sea—Baltic Sea model (Gräwe et al., 2015) to provide a mean annual cycle of daily temperature, salinity, and sea surface height here. A quadratic polynomial fitted to the timeseries of GCM temperature and salinity at or close to the Baltic boundary is used to add a climate change single to the present day mean annual cycle. The sea surface height gradient between the northern and Baltic open boundaries is corrected to match that in a high resolution reanalysis forced global ocean model (Duchez et al., 2014). No climate change signal in this gradient is included here.

The simulations are run from rest at 1980 out to 2095; the first three years are treated as spin-up and not included in further analysis. A single, business as usual without mitigation emissions scenario (RCP8.5) is used. To define

the climate change signal, we consider mean annual cycles at daily frequency or boreal summer (June–September) mean values, both averaged over 30-year periods, comparing 2066–2095 (Future) with 1983–2012 (Present).

2.3. Potential Energy Anomaly Analysis

The PEA provides a useful metric for seasonal stratification, being an integral property not dependent on thresholds and supported by a theory for its evolution. Here we consider the PEA density deficit (but just referred to as PEA; J m^{-3}), defined by:

$$\phi = -\frac{g}{h} \int_{z=-h}^{0} z\Big(\rho(T,S) - \rho\big(\overline{T},\overline{S}\big)\Big) dz \tag{1}$$

Overbars indicate depth mean and all integrations are limited to 200 m depth. Here z is positive-upwards vertical coordinate, h the water depth (limited to 200 m), T the potential temperature (°C), S the salinity (PSU), ρ the potential density, and g the gravitational acceleration. The analysis uses daily mean model output throughout. The PEA is zero for a fully mixed water column and becomes increasingly positive for strengthening stratification. Simpson and Bowers (1981) provide a simple model for PEA temporal evolution:

$$\frac{d\phi}{dt} = B_H + R \tag{2a}$$

$$B_H = \frac{\alpha g Q}{2c_p} \tag{2b}$$

So

$$\phi(t) = \int_{t_0}^{t} B_H + R \, dt' + \phi(t_0) \tag{3}$$

Where R is a residual term described below, α is the thermal expansivity, Q (W m^{-2}) is the positive downward surface heat-flux and C_p (J kg^{-1}°C^{-1}) the specific heat capacity. Here we use the EOS-80 equation of state throughout (rather than the more recent TEOS-10) to maintain consistency with the model simulations. The start of the integration t_0 is defined such that $\phi(t_0) = 0$. The PEA is decomposed into a surface heat flux component (ϕ_{qt}) and a residual component (ϕ_R). The surface heat-flux component is further subdivided into:

$$\int_{t_0}^{t} B_H dt' = \phi_{qt} = \phi_{qsr} + \phi_{qns} \;\; \text{with} \; \phi_{qns} = \phi_{qsb} + \phi_{qla} + \phi_{qlw} \tag{4}$$

representing respectively: total heat-flux, shortwave solar and non-solar (being made up of sensible, latent, and longwave) heat-flux components. Equation 4 is integrated forward from 1 January each year with a daily time-step and reset to zero whenever the integral is less than zero. This both accounts for the overturning of the water column on net-negative buoyancy forcing (not otherwise treated here) and alleviates the need to specify an arbitrary t_0.

The residual component of the PEA, ϕ_R, is a combination of surface freshwater forcing, advective induced stratification (positive) and wind and tidal mixing (negative). A complete decomposition of these terms is available (Burchard & Hofmeister, 2008), however, this is not considered further here not least because the data required to calculate the full expression was not saved in these model simulations, and resorting to empirical expressions for tidal and wind mixing (Simpson & Bowers, 1981) adds an unnecessarily element of uncertainty. Instead, we calculate $\phi_R = \phi - \phi_{qt}$.

2.4. Model Uncertainty Analysis

To provide some reassurance that the climate model forced simulations provide a realistic representation of present-day conditions we conduct a comparison with a monthly climatology of the EN4 temperature and salinity profile data set (Good et al., 2013) constructed on the model grid (Figure 1; see Table S3 in Supporting

Information S1 for details). Considering PEA, the salinity component of PEA (PEAS; see text around Figure S2 in Supporting Information S1) and sea surface temperature (SST), we can readily identify four ensemble members that fail to reproduce acceptable present-day conditions. Three (HadGEM2-CC, HadGEM2-ES, and IPSL-CM5B-LR) show unrealistic levels of (year-round) salinity stratification, arising from biases in the open-ocean boundary conditions, and one (BCC-CSM1-1-m) shows unrealistically low summertime stratification (Table S3 and Figure S1 in Supporting Information S1). These four models are excluded from further analysis, and we focus on the remaining seven "core" ensemble members. To put the performance of these simulations in context we compare with a reanalysis (ERA-Interim) forced simulation of the same model configuration (from 1980 to 2015; SSB-Hind, corresponding to run ST in (Luneva et al., 2019)). PEA spatial correlations range 0.81–0.84 for the seven core members, compared with 0.85 for SSB-Hind; cost function (χ) from 0.58 to 0.64 c.f. 0.54 for SSB-Hind; and mean error -0.08–14.38 J m^{-3} c.f. -7.73 J m^{-3} for SSB-Hind. Ranking the models for all the metrics considered on-shelf, SSB-Hind is the second most accurate. Hence, while there is some degradation when climate model forcing is used this is quite minor for these core members.

3. Results

3.1. Future Views of Stratification in the Northwest European Shelf Seas

Our ensemble of downscale future climate simulations shows the expected pattern of on-shelf summertime (June–September) stratification for core members (Figure 1), with values typically 50–100 J m^{-3}. Regions less than 25 J m^{-3} can be interpreted as well mixed throughout the year. In deep water the results are more variable, most likely reflecting the importance of salinity stratification here, which is less well represented in the GCMs.

The simulations show a consistent increase in PEA across the Northwest European shelf seas between present day and future conditions (Figure 2). There are large variations between ensemble members, but in no case are there large areas of decreasing PEA. Changes in the shelf seas are generally weaker than in the open ocean, reflecting the annual reset of stratification by the full-depth winter mixing each year. In all ensemble members except one, the differences in summer PEA are uniformly significant at the 99% confidence level. The GFDL-ESM2M forced simulation only shows a significant positive change over shelf sea regions in the central and northern North Sea. In several members there is a very strong increase in the PEA in frontal and well mixed regions, indicating an expansion of the stratified regions as the balance in Equation 2a becomes positive. We ascertain the nature of this increase in PEA (Figures S2 and S3 in Supporting Information S1) by recalculating with depth-mean salinity (Holt et al., 2010). This clearly shows temperature dominates the change on-shelf and salinity dominates it in the open ocean. This demonstrates these shelf seas are isolated from the intense increases in salinity stratification seen here in the NE Atlantic (Figure S3 in Supporting Information S1). Generally, ocean-shelf transport and shelf sea circulation are too slow, compared with the annual mixing cycle, to support an advective increase in salinity stratification in the shelf sea regions.

The evolution of PEA is explained through the integration of Equation 2a, as a sum of solar (ϕ_{qsr}) and non-solar (ϕ_{qns}) heat-flux terms, and a residual (ϕ_R). Exploring the terms (Figure 3) for an example region and ensemble members showing smallest (GFDL-ESM2M) and largest (MIROC-ESM) PEA increase, demonstrates that stratification in these seas is a delicate balance of heating, heat-loss and mixing. The resultant PEA being much smaller than the driving terms. Into the future, in both cases the solar heat-flux term (ϕ_{qsr}), becomes more positive, the non-solar heat-flux (ϕ_{qns}) and the residual (mixing) terms more negative, with a net positive change in both the total heat-flux term (ϕ_{qt}) and PEA. The heat-flux terms are proportional to the thermal expansivity (Equation 2b), which itself increases with temperature, for example, at 10°C a 2°C increase in temperature gives a 12% increase in expansivity (see Figure S4 in Supporting Information S1 for maps of fractional change in expansivity). The dominance of this expansivity variation is apparent when the calculation is repeated with the expansivity held constant at mean present-day values. Now in the GFDL-ESM2M case the solar radiation term (ϕ_{qsr}) decreases slightly and the total heat-flux remains approximately constant. In the MIROC-ESM case the increase in the solar radiation and total terms are both significantly reduced, but still positive.

Turning to changes in PEA in the full ensemble and in all regions (Figure 4), the shortwave radiation component (ϕ_{qsr}) is the only consistently increasing driving term; ϕ_{qsr} increases for all regions and all ensemble members, except for the CanESM2 model in western regions where it is weakly negative. This is not to say that solar radiation is increasing in all these cases; this is a much more nuanced aspect of climate change relating to highly
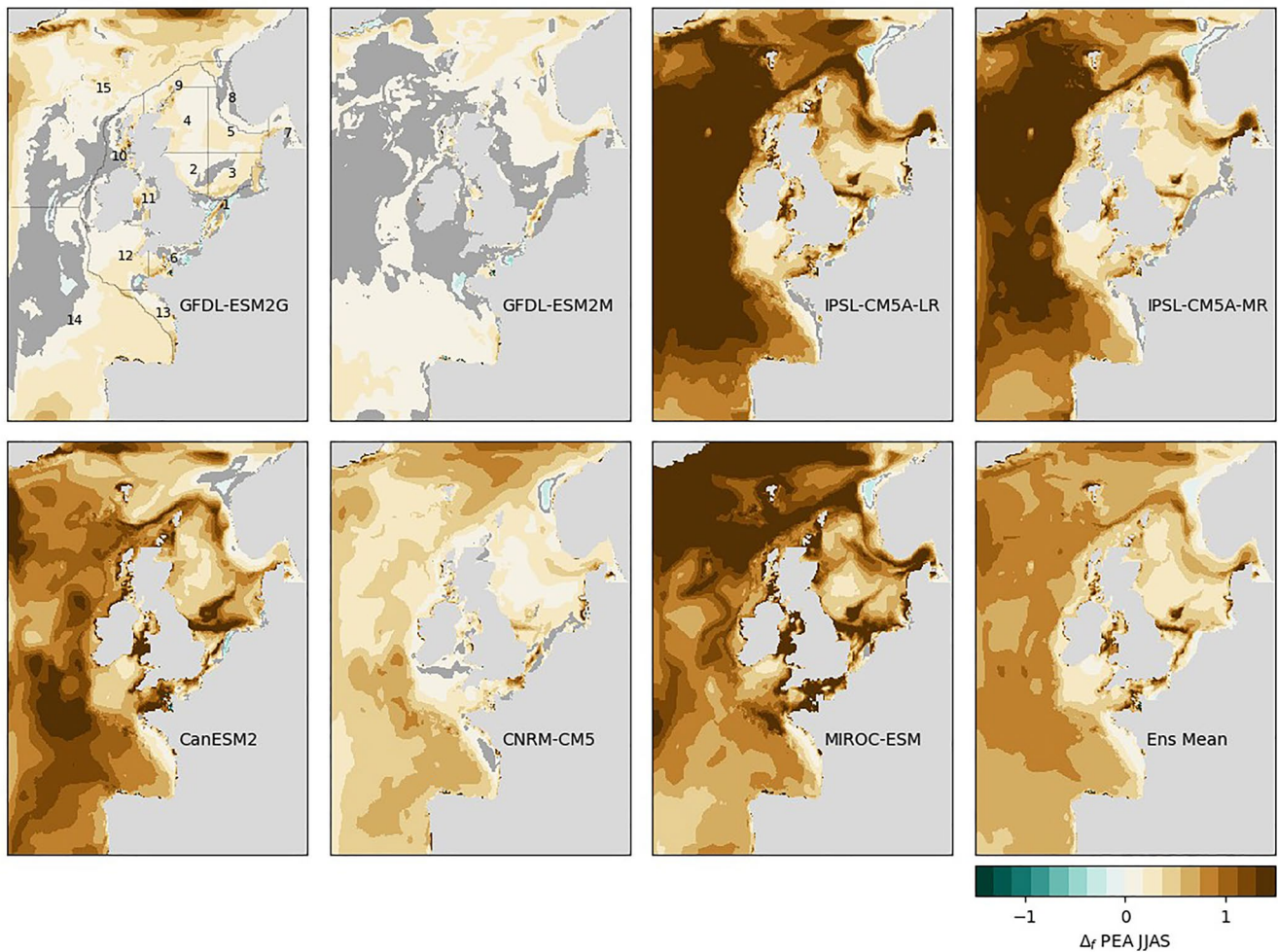
Figure 2. Fractional change in summer stratification for the core ensemble members from future (2066–2095) to present-day period (1983–2012), also shown is the change in ensemble mean. Areas where the difference is not significant at 99% confidence compared with interannual variability are shaded out in dark gray. This uses the Kruskal–Wallis test (Kruskal & Wallis, 1952). Top-left panel shows regions used for area averages.

uncertain changes in cloud cover. Instead, that solar heating is positive definite and the expansivity that acts on it is consistently increasing, through its dependence on temperature. The change in sensible heat-flux term (ϕ_{qsb}) is close to zero in all cases, supporting the comment in the introduction that a change in air temperature is not able to drive a change in seasonal stratification in this context. Changes in latent (ϕ_{qla}) and longwave (ϕ_{qlw}) heat-flux terms are small and negative, both driven by increases in SST. Changes in the residual term are highly variable, largely reflecting changes in wind speed (noting changes to tidal currents due to sea level variations are not included in these simulations), and advective components (e.g., in the Norwegian Trench). It is interesting to note that in the open ocean regions of this model, the strong increase in stratification is driven by the residual term, here interpreted as an advective component, reflecting changes in surface salinity in the wider Atlantic, Nordic Seas, and Arctic (Figure S3 in Supporting Information S1 and Holt et al., 2018).

The importance of the expansivity can be confirmed by, again, repeating the calculation with constant α. Focusing on the ensemble mean, the shortwave term with constant α is close to zero in all regions, confirming there is not a consistent change in solar forcing in this CMIP5 ensemble (except in the Irish Sea). Moreover, the total ($\Delta\phi_{qt}$) is greatly reduced in all regions where there is substantial seasonal stratification. While the change in total buoyancy forcing ($\Delta\phi_{qt}$) is positive for all regions and ensemble members in the original calculation, it becomes negative for 41% of regions and ensemble members when recalculated with a constant expansivity. Hence, changes in heat-flux terms are highly variable (with driving model and region), but the positive definite change in thermal expansivity is sufficient for them to all show consistently positive changes in buoyancy forcing.
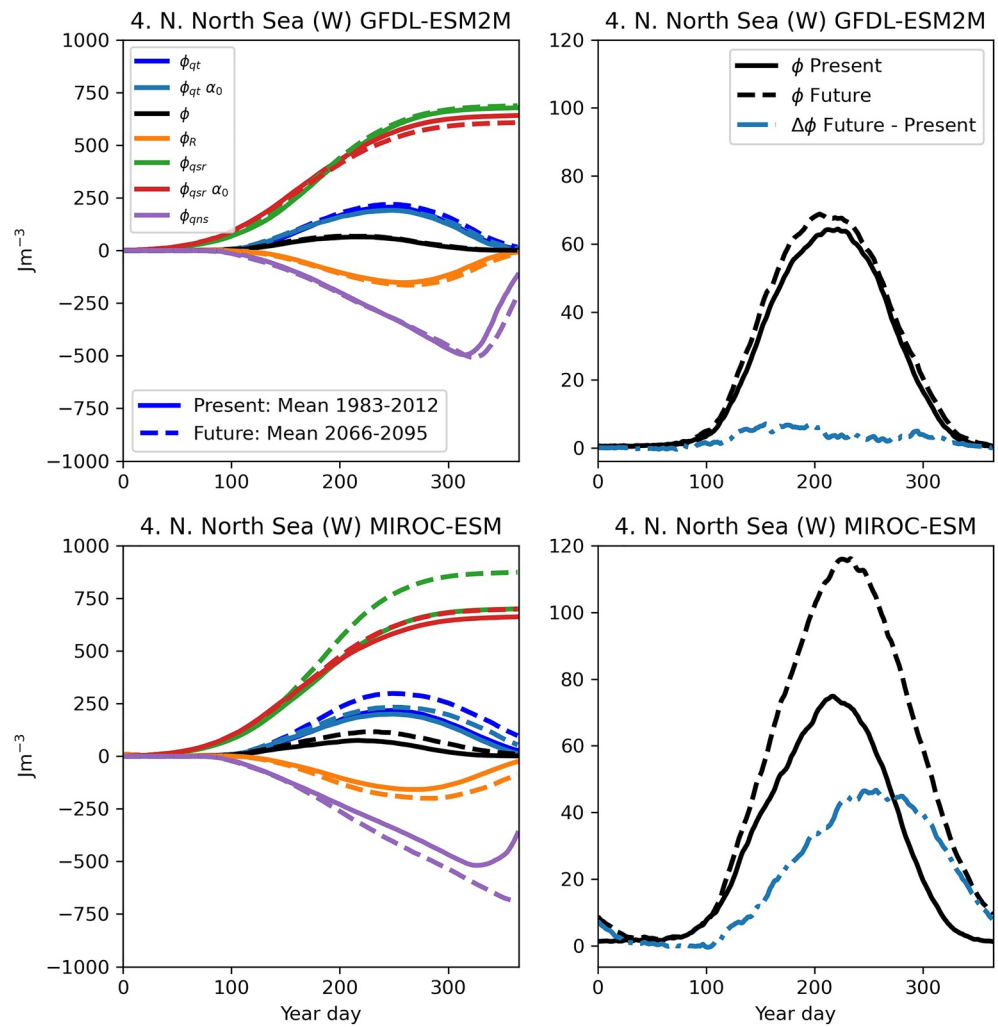
Figure 3. Mean annual cycle in potential energy anomaly (PEA) (right) and terms driving it (left; Equations 3 and 4; i.e., PEA (ϕ), is decomposed into total heat-flux (ϕ_{qt}) and residual ϕ_R terms, and ϕ_{qt} into solar (ϕ_{qsr}) and non-solar (ϕ_{qns}) terms) for the Northern North Sea (west) region and the ensemble members showing the smallest (top) and largest (bottom) overall summer PEA change. Also shown are the total heat-flux term (ϕ_{qt}) and the shortwave radiation term (ϕ_{qsr}) recalculated with thermal expansivity held at the annual mean present-day value ($\alpha 0$). Values are averaged over seasonally stratified regions in each year, that is, minimum PEA < 25 J m^{-3} and maximum PEA > 25 J m^{-3}. The Northern North Sea (west) region is almost entirely seasonally stratified, with small well-mixed coastal areas, which shrink in the future time period (See Figure S5 in Supporting Information S1).

While the changes in expansivity are relatively small (Figure S4 in Supporting Information S1), because buoyancy input is closely balanced by mixing, a small increase in buoyancy leads to a (proportionately) larger increase in PEA. Hence there is an amplification of the stratification response to buoyancy forcing. Averaged across seasonally stratified shelf sea regions and ensemble members the fractional increase in PEA is about 2.0 times the increase in buoyancy input.

4. Discussion and Conclusions

The straightforward answer to the question posed in the title of this paper is that if sea temperatures are expected to increase as a robust response to global heating by increased atmospheric greenhouse gas concentrations, then so will the buoyancy forcing that drives seasonal stratification. This is not dependent on any seasonal change in heat-flux or mixing but just the increase in thermal expansivity with temperature, and the multiannual increase in net surface and lateral heat-flux that leads to this increase in sea temperature. On the face of it the increase in
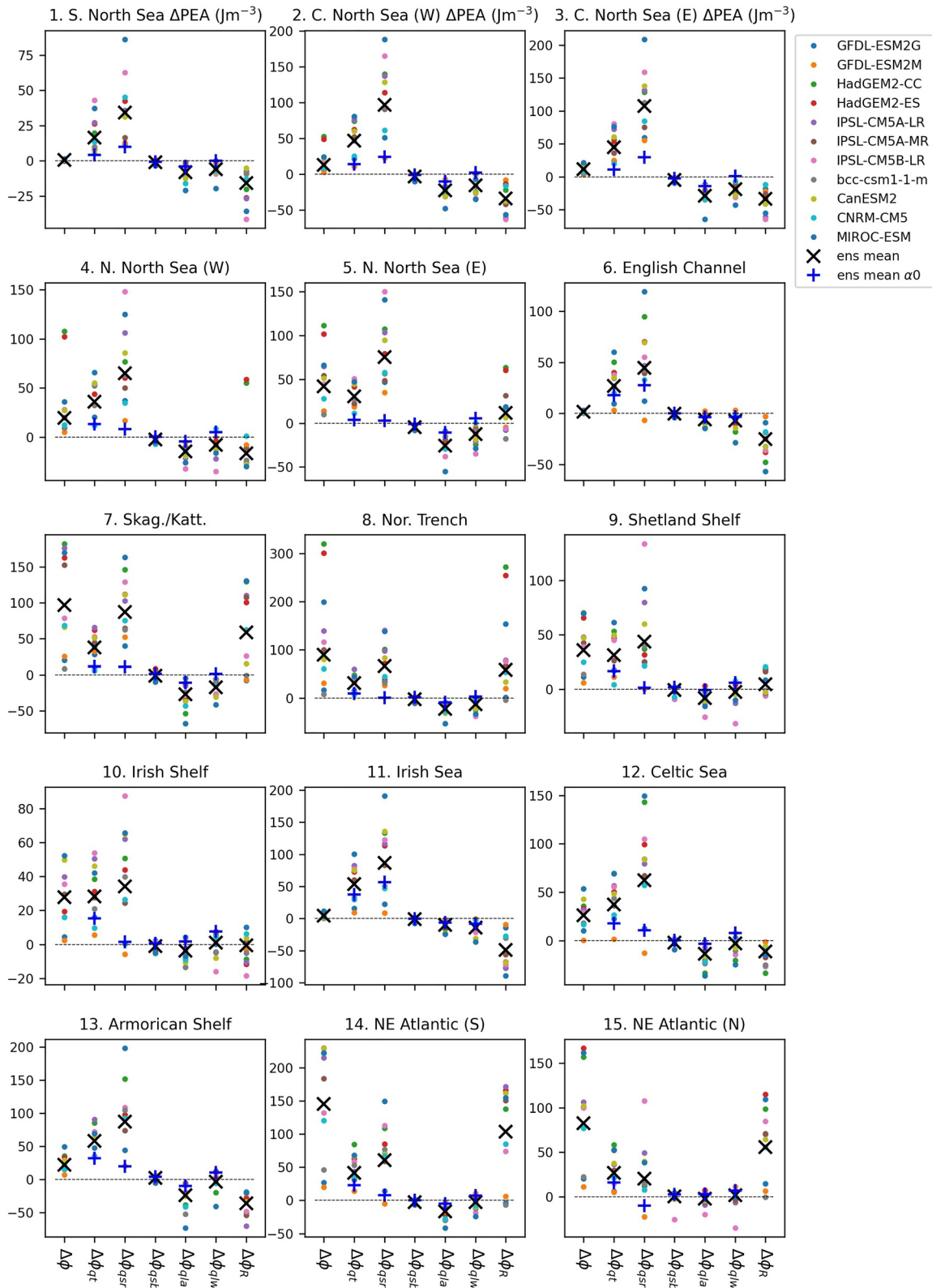
Figure 4. Change in summer mean potential energy anomaly (PEA) and driving terms (Equations 3 and 4) between 1983–2012 and 2066–2095. (X) Shows core ensemble mean (excluding 4 members) and (+) shows this mean recalculated with expansivity held at annual mean present-day values ($\alpha 0$). Values are averaged over each region, excluding well mixed areas (i.e., maximum PEA > 25 J m^{-3}).

buoyancy forcing from expansivity is comparatively small. However, when the seasonal stratification arises from a close balance between buoyancy forcing and mixing then this effect is amplified. While the sign of the change in sea temperature is clear, the response of sea temperatures to changes in atmospheric conditions is highly uncertain, relating to both heat-fluxes and shelf-sea circulation (Holt et al., 2010). For example, there is a large range in air-temperature changes over regions and ensemble members considered here (from 1.9°C to 6.0°C) and the ratio of SST change to air temperature change ranges from 0.15 to 0.78. This uncertainty translates to uncertainty in expansivity and buoyancy forcing.

We can infer many biogeochemical implications for this increase in seasonal stratification; noting that these are all highly nuanced and context dependent and deserve a more thorough investigation than can be provided here. An increase in buoyancy forcing would generally imply buoyancy overcomes mixing earlier in the spring; this is apparent in Figure 3 and demonstrated in Figure S5 in Supporting Information S1. This shows on-shelf the seasonal stratification occurs earlier by ~11 days. Interestingly, frontal regions show a considerable delay in stratification on-set, presumably due to increased wind mixing, which deserves further investigation. Earlier and stronger stratification onset would imply earlier spring phytoplankton blooms, these might be expected to be less intense when seasonal light limitation or nutrient resupply are a factor.

Increased summer-time stratification would tend to reduce diapycnal mixing through reduced shear-generated turbulence. However, an increase in internal-wave energy and consequent pycnocline mixing (e.g., Sharples & Zeldis, 2021) is an potentially important negative feedback of the stratification increase, not captured by this model due to limited horizontal resolution. Similarly, stronger vertical gradients, would tend to counter effects of reduced mixing on vertical fluxes. Hence, it is quite uncertain how this increase in stratification would affect the upward nutrient flux into the thermocline, which fuels mid-water production. This would also be highly sensitive to whether mixing depths are also decreased through the increase in buoyancy forcing. Projections of future mixing states are further complicated by the effects of human action, specifically the potentially significant increase in off-shore wind generation in stratified waters and its local consequences for mixing (Dorrell et al., 2022). At tidal mixing fronts the strength of horizontal density gradients is expected to increase with the vertical density gradient on the stratified side of the front, and so increase the strength of the corresponding density driven circulation (Hill et al., 2008); important for the transport of larvae and pollutants.

We currently lack a detailed picture of the stratification-mixing regime of the coastal ocean around the world, from either an observational or modeling standpoint. However, we can identify several mid-latitude coastal-ocean regions, which exhibit seasonal stratification driven by the balance between seasonal variations of surface heating and mixing, and so where the analysis in this paper is likely to be directly relevant. These include: Gulf of Alaska, California Current, Gulf of California, NE US continental shelf, Scotian Shelf, Newfoundland-Labrador shelf, Patagonian Shelf, East China Seas, East/Japan Sea, Yellow Sea, Sea of Okhotsk, and New Zealand shelf (here we use the NOAA Large Marine Ecosystem nomenclature). We have excluded Arctic seas here both because ice cover will radically change the seasonal dynamics and also the because the expansivity is very small in these cases. There is another class of, generally tropical and sub-tropical, seas where seasonality is controlled by monsoonal variations of wind mixing, with a comparatively steady buoyancy forcing. Whether the arguments here (with seasonally varying heating and comparatively steady mixing) are symmetric in this respect deserves closer analysis.

Hence, we can conclude that increasing stratification strength in seasonally stratified seas is a robust impact of global heating. This will be modulated by changes in mixing, for example, by winds and convection, and changes in freshwater input and circulation, which will all be less certain, highly context dependent and have either positive or negative effects. However, the underlying, surface heating driven term is expected to be increasing.

Data Availability Statement

References

Breitburg, D., Levin, L. A., Oschlies, A., Gregoire, M., Chavez, F. P., Conley, D. J., et al. (2018). Declining oxygen in the global ocean and coastal waters. *Science*, *359*(6371), eaam7240. https://doi.org/10.1126/science.aam7240

Burchard, H., & Hofmeister, R. (2008). A dynamic equation for the potential energy anomaly for analysing mixing and stratification in estuaries and coastal seas. *Estuarine, Coastal and Shelf Science*, *77*(4), 679–687. https://doi.org/10.1016/j.ecss.2007.10.025

Dorrell, R. M., Lloyd, C. J., Lincoln, B. J., Rippeth, T. P., Taylor, J. R., Caulfield, C. C. P., et al. (2022). Anthropogenic mixing in seasonally stratified shelf seas by offshore wind farm infrastructure. *Frontiers in Marine Science*, *9*. https://doi.org/10.3389/fmars.2022.830927

Drenkard, E. J., Stock, C., Ross, A. C., Dixon, K. W., Adcroft, A., Alexander, M., et al. (2021). Next-generation regional ocean projections for living marine resource management in a changing climate. *ICES Journal of Marine Science*, *78*(6), 1969–1987. https://doi.org/10.1093/icesjms/fsab100

Duchez, A., Frajka-Williams, E., Castro, N., Hirschi, J., & Coward, A. (2014). Seasonal to interannual variability in density around the Canary Islands and their influence on the Atlantic meridional overturning circulation at 26°N. *Journal of Geophysical Research: Oceans*, *119*(3), 1843–1860. https://doi.org/10.1002/2013jc009416

Fernand, L., Weston, K., Morris, T., Greenwood, N., Brown, J., & Jickells, T. (2013). The contribution of the deep chlorophyll maximum to primary production in a seasonally stratified shelf sea, the North Sea. *Biogeochemistry*, *113*(1–3), 153–166. https://doi.org/10.1007/s10533-013-9831-7

Good, S. A., Martin, M. J., & Rayner, N. A. (2013). EN4: Quality controlled ocean temperature and salinity profiles and monthly objective analyses with uncertainty estimates. *Journal of Geophysical Research: Oceans*, *118*(12), 6704–6716. https://doi.org/10.1002/2013jc009067

Gräwe, U., Holtermann, P., Klingbeil, K., & Burchard, H. (2015). Advantages of vertically adaptive coordinates in numerical models of stratified shelf seas. *Ocean Modelling*, *92*, 56–68. https://doi.org/10.1016/j.ocemod.2015.05.008

Hickman, A. E., Moore, C. M., Sharples, J., Lucas Mi, T. G. H., Krivtsov, V., & Holligan, P. M. (2012). Primary production and nitrate uptake within the seasonal thermocline of a stratified shelf sea. *Marine Ecology Progress Series*, *463*, 39–57. https://doi.org/10.3354/meps09836

Hill, A. E., Brown, J., Fernand, L., Holt, J., Horsburgh, K. J., Proctor, R., et al. (2008). Thermohaline circulation of shallow tidal seas. *Geophysical Research Letters*, *35*(11), L11605. https://doi.org/10.1029/2008gl033459

Holt, J., Hyder, P., Ashworth, M., Harle, J., Hewitt, H. T., Liu, H., et al. (2017). Prospects for improving the representation of coastal and shelf seas in global ocean models. *Geoscientific Model Development*, *10*(1), 499–523. https://doi.org/10.5194/gmd-10-499-2017

Holt, J., Polton, J., Huthnance, J., Wakelin, S., O'Dea, E., Harle, J., et al. (2018). Climate-driven change in the North Atlantic and Arctic Oceans can greatly reduce the circulation of the North Sea. *Geophysical Research Letters*, *45*(21), 11827–11836. https://doi.org/10.1029/2018GL078878

Holt, J., Schrum, C., Cannaby, H., Daewel, U., Allen, I., Artioli, Y., et al. (2016). Potential impacts of climate change on the primary production of regional seas: A comparative analysis of five European seas. *Progress in Oceanography*, *140*, 91–115. https://doi.org/10.1016/j.pocean.2015.11.004

Holt, J., Wakelin, S., Lowe, J., & Tinker, J. (2010). The potential impacts of climate change on the hydrography of the northwest European continental shelf. *Progress in Oceanography*, *86*(3–4), 361–379. https://doi.org/10.1016/j.pocean.2010.05.003

Kruskal, W. H., & Wallis, W. A. (1952). Use of ranks in one-criterion variance analysis. *Journal of the American Statistical Association*, *47*(260), 583–621. https://doi.org/10.1080/01621459.1952.10483441

Large, W. G., & Yeager, S. (2004). Diurnal to decadal global forcing for ocean and sea-ice models: The data sets and flux climatologies. NCAR Technical Note. *National Center for Atmospheric Research*, *11*, 324–336. NCAR/TN-460+STR. https://doi.org/10.5065/D6KK98Q6

Legge, O., Johnson, M., Hicks, N., Jickells, T., Diesing, M., Aldridge, J., et al. (2020). Carbon on the northwest European shelf: Contemporary budget and future influences. *Frontiers in Marine Science*, *7*, 143. https://doi.org/10.3389/fmars.2020.00143

Luneva, M. V., Wakelin, S., Holt, J. T., Inall, M. E., Kozlov, I. E., Palmer, M. R., et al. (2019). Challenging vertical turbulence mixing schemes in a tidally energetic environment: 1. 3-D shelf-sea model assessment. *Journal of Geophysical Research: Oceans*, *124*(8), 6360–6387. https://doi.org/10.1029/2018jc014307

O'Dea, E., Furner, R., Wakelin, S., Siddorn, J., While, J., Sykes, P., et al. (2017). The CO5 configuration of the 7 km Atlantic Margin Model: Large-scale biases and sensitivity to forcing, physics options and vertical resolution. *Geoscientific Model Development*, *10*(8), 2947–2969. https://doi.org/10.5194/gmd-10-2947-2017

Queste, B. Y., Fernand, L., Jickells, T. D., Heywood, K. J., & Hind, A. J. (2016). Drivers of summer oxygen depletion in the central North Sea. *Biogeosciences*, *13*(4), 1209–1222. https://doi.org/10.5194/bg-13-1209-2016

Rippeth, T. P., Lincoln, B. J., Kennedy, H. A., Palmer, M. R., Sharples, J., & Williams, C. A. J. (2014). Impact of vertical mixing on sea surface pCO_2 in temperate seasonally stratified shelf seas. *Journal of Geophysical Research: Oceans*, *119*(6), 3868–3882. https://doi.org/10.1002/2014JC010089

Ruiz-Castillo, E., Sharples, J., & Hopkins, J. (2019). Wind-driven strain extends seasonal stratification. *Geophysical Research Letters*, *46*(22), 13244–13252. https://doi.org/10.1029/2019GL084540

Sharples, J., & Zeldis, J. R. (2021). Variability of internal tide energy, mixing and nitrate fluxes in response to changes in stratification on the northeast New Zealand continental shelf. *New Zealand Journal of Marine & Freshwater Research*, *55*(1), 94–111. https://doi.org/10.1080/00288330.2019.1705357

Simpson, J. H., & Bowers, D. (1981). Models of stratification and frontal movement in shelf seas. *Deep-Sea Research*, *28*(7), 727–738. https://doi.org/10.1016/0198-0149(81)90132-1

Taylor, K. E., Stouffer, R. J., & Meehl, G. A. (2012). An overview of CMIP5 and the experiment design. *Bulletin of the American Meteorological Society*, *93*(4), 485–498. https://doi.org/10.1175/BAMS-D-11-00094.1

Tinker, J., Lowe, J., Pardaens, A., Holt, J., & Barciela, R. (2016). Uncertainty in climate projections for the 21st century northwest European shelf seas. *Progress in Oceanography*, *148*, 56–73. https://doi.org/10.1016/j.pocean.2016.09.003

Topcu, H. D., & Brockmann, U. H. (2015). Seasonal oxygen depletion in the North Sea, a review. *Marine Pollution Bulletin*, *99*(1–2), 5–27. https://doi.org/10.1016/j.marpolbul.2015.06.021

Umlauf, L., & Burchard, H. (2003). A generic length-scale equation for geophysical turbulence models. *Journal of Marine Research*, *61*(2), 235–265. https://doi.org/10.1357/002224003322005087

Vörösmarty, C. J., Fekete, B. M., Meybeck, M., & Lammers, R. B. (2000). Global system of rivers: Its role in organizing continental land mass and defining land-to-ocean linkages. *Global Biogeochemical Cycles*, *14*(2), 599–621. https://doi.org/10.1029/1999gb900092

Wihsgott, J. U., Sharples, J., Hopkins, J. E., Woodward, E. M. S., Hull, T., Greenwood, N., & Sivyer, D. B. (2019). Observations of vertical mixing in autumn and its effect on the autumn phytoplankton bloom. *Progress in Oceanography*, *177*, 102059. https://doi.org/10.1016/j.pocean.2019.01.001

Young, E. F., & Holt, J. T. (2007). Prediction and analysis of long-term variability of temperature and salinity in the Irish Sea. *Journal of Geophysical Research*, *112*(C1), C01008. https://doi.org/10.1029/2005JC003386

References From the Supporting Information

Adlandsvik, B. (2008). Marine downscaling of a future climate scenario for the North Sea. *Tellus A: Dynamic Meteorology and Oceanography*, *60*(3), 451–458. https://doi.org/10.1111/j.1600-0870.2007.00311.x

Alexander, M. A., Shin, S.-I., Scott, J. D., Curchitser, E., & Stock, C. (2020). The response of the Northwest Atlantic Ocean to climate change. *Journal of Climate*, *33*(2), 405–428. https://doi.org/10.1175/JCLI-D-19-0117.1

Arellano, B., & Rivas, D. (2019). Coastal upwelling will intensify along the Baja California coast under climate change by mid-21st century: Insights from a GCM-nested physical-NPZD coupled numerical ocean model. *Journal of Marine Systems*, *199*, 103207. https://doi.org/10.1016/j.jmarsys.2019.103207

Brochier, T., Echevin, V., Tam, J., Chaigneau, A., Goubanova, K., & Bertrand, A. (2013). Climate change scenarios experiments predict a future reduction in small pelagic fish recruitment in the Humboldt Current system. *Global Change Biology*, *19*(6), 1841–1853. https://doi.org/10.1111/gcb.12184

Cannaby, H., Fach, B. A., Arkin, S., & Salihoglu, B. (2015). Climatic controls on biophysical interactions in the Black Sea under present day conditions and a potential future (A1B) climate scenario. *Journal of Marine Systems*, *141*, 149–166. https://doi.org/10.1016/j.jmarsys.2014.1008.1005

Chamberlain, M. A., Sun, C., Matear, R. J., Feng, M., & Phipps, S. J. (2012). Downscaling the climate change for oceans around Australia. *Geoscientific Model Development*, *5*(5), 1177–1194. https://doi.org/10.5194/gmd-5-1177-2012

Chylek, P., Li, J., Dubey, M. K., Wang, M., & Lesins, G. (2011). Observed and model simulated 20th century Arctic temperature variability: Canadian Earth system model CanESM2. *Atmospheric Chemistry and Physics Discussions*, *2011*, 22893–22907. https://doi.org/10.5194/acpd-11-22893-2011

Collins, W. J., Bellouin, N., Doutriaux-Boucher, M., Gedney, N., Halloran, P., Hinton, T., et al. (2011). Development and evaluation of an Earth-System model – HadGEM2. *Geoscientific Model Development*, *4*(4), 1051–1075. https://doi.org/10.5194/gmd-4-1051-2011

Cordeiro Pires, A., Nolasco, R., Rocha, A., Ramos, A. M., & Dubert, J. (2016). Climate change in the Iberian upwelling system: A numerical study using GCM downscaling. *Climate Dynamics*, *47*(1), 451–464. https://doi.org/10.1007/s00382-015-2848-y

Dieterich, C., Wang, S., Schimanke, S., Groger, M., Klein, B., Hordoir, R., et al. (2019). Surface heat budget over the North Sea in climate change simulations. *Atmosphere*, *10*(5), 272. https://doi.org/10.3390/atmos10050272

Dufresne, J. L., Foujols, M. A., Denvil, S., Caubel, A., Marti, O., Aumont, O., et al. (2013). Climate change projections using the IPSL-CM5 Earth system model: From CMIP3 to CMIP5. *Climate Dynamics*, *40*(9), 2123–2165. https://doi.org/10.1007/s00382-012-1636-1

Dunne, J. P., John, J. G., Adcroft, A. J., Griffies, S. M., Hallberg, R. W., Shevliakova, E., et al. (2012). GFDL's ESM2 global coupled climate–carbon Earth system models. Part I: Physical formulation and baseline simulation characteristics. *Journal of Climate*, *25*(19), 6646–6665. https://doi.org/10.1175/JCLI-D-11-00560.1

Echevin, V., Gévaudan, M., Espinoza-Morriberón, D., Tam, J., Aumont, O., Gutierrez, D., & Colas, F. (2020). Physical and biogeochemical impacts of RCP8.5 scenario in the Peru upwelling system. *Biogeosciences*, *17*(12), 3317–3341. https://doi.org/10.5194/bg-17-3317-2020

Echevin, V., Goubanova, K., Belmadani, A., & Dewitte, B. (2012). Sensitivity of the Humboldt current system to global warming: A downscaling experiment of the IPSL-CM4 model. *Climate Dynamics*, *38*(3–4), 761–774. https://doi.org/10.1007/s00382-011-1085-2

Friocourt, Y. F., Skogen, M., Stolte, W., & Albretsen, J. (2012). Marine downscaling of a future climate scenario in the North Sea and possible effects on dinoflagellate harmful algal blooms. *Food Additives & Contaminants Part a-Chemistry Analysis Control Exposure & Risk Assessment*, *29*(10), 1630–1646. https://doi.org/10.1080/19440049.2012.714079

Gräwe, U., Friedland, R., & Burchard, H. (2013). The future of the western Baltic Sea: Two possible scenarios. *Ocean Dynamics*, *63*(8), 901–921. https://doi.org/10.1007/s10236-013-0634-0

Gröger, M., Arneborg, L., Dieterich, C., Höglund, A., & Meier, H. E. M. (2019). Summer hydrographic changes in the Baltic Sea, Kattegat and Skagerrak projected in an ensemble of climate scenarios downscaled with a coupled regional ocean–sea ice–atmosphere model. *Climate Dynamics*, *53*(9), 5945–5966. https://doi.org/10.1007/s00382-019-04908-9

Gröger, M., Maier-Reimer, E., Mikolajewicz, U., Moll, A., & Sein, D. (2013). NW European shelf under climate warming: Implications for open ocean and shelf exchange, primary production, and carbon absorption. *Biogeosciences*, *10*(6), 3767–3792. https://doi.org/10.5194/bg-10-3767-2013

Han, G., Ma, Z., Long, Z., Perrie, W., & Chassé, J. (2018). Climate change on Newfoundland and labrador shelves: Results from a regional downscaled ocean and sea-ice model under an A1B forcing scenario 2011–2069. *Atmosphere-Ocean*, *57*(1), 3–17. https://doi.org/10.1080/07055900.2017.1417110

Hermann, A. J., Gibson, G. A., Cheng, W., Ortiz, I., Aydin, K., Wang, M., et al. (2019). Projected biophysical conditions of the Bering Sea to 2100 under multiple emission scenarios. *ICES Journal of Marine Science*, *76*(5), 1280–1304. https://doi.org/10.1093/icesjms/fsz043

Holdsworth, A. M., Zhai, L., Lu, Y., & Christian, J. R. (2021). Future changes in oceanography and Biogeochemistry along the Canadian Pacific continental margin. *Frontiers in Marine Science*, *8*, 602991. https://doi.org/10.3389/fmars.2021.602991

Holt, J., Butenschon, M., Wakelin, S. L., Artioli, Y., & Allen, J. I. (2012). Oceanic controls on the primary production of the Northwest European continental shelf: Model experiments under recent past conditions and a potential future scenario. *Biogeosciences*, *9*(1), 97–117. https://doi.org/10.5194/bg-9-97-2012

Howard, E. M., Frenzel, H., Kessouri, F., Renault, L., Bianchi, D., McWilliams, J. C., & Deutsch, C. (2020). Attributing causes of future climate change in the California current system with multimodel downscaling. *Global Biogeochemical Cycles*, *34*(11), e2020GB006646. https://doi.org/10.1029/2020GB006646

Kay, S., & Butenschön, M. (2018). Projections of change in key ecosystem indicators for planning and management of marine protected areas: An example study for European seas. *Estuarine, Coastal and Shelf Science*, *201*, 172–184. https://doi.org/10.1016/j.ecss.2016.03.003

Mathis, M., Elizalde, A., & Mikolajewicz, U. (2018). Which complexity of regional climate system models is essential for downscaling anthropogenic climate change in the Northwest European Shelf? *Climate Dynamics*, *50*(7), 2637–2659. https://doi.org/10.1007/s00382-017-3761-3

Mathis, M., Elizalde, A., & Mikolajewicz, U. (2019). The future regime of Atlantic nutrient supply to the Northwest European Shelf. *Journal of Marine Systems*, *189*, 98–115. https://doi.org/10.1016/j.jmarsys.2018.10.002

Mathis, M., & Pohlmann, T. (2014). Projection of physical conditions in the North Sea for the 21st century. *Climate Research*, *61*(1), 1–17. https://doi.org/10.3354/cr01232

Meier, H. E. M. (2006). Baltic Sea climate in the late twenty-first century: A dynamical downscaling approach using two global models and two emission scenarios. *Climate Dynamics*, *27*(1), 39–68. https://doi.org/10.1007/s00382-006-0124-x

Misra, V., Mishra, A., & Bhardwaj, A. (2019). A coupled ocean-atmosphere downscaled climate projection for the peninsular Florida region. *Journal of Marine Systems*, *194*, 25–40. https://doi.org/10.1016/j.jmarsys.2019.02.010

Moore, S. K., Johnstone, J. A., Banas, N. S., & Salathé, E. P. (2015). Present-day and future climate pathways affecting Alexandrium blooms in Puget Sound, WA, USA. *Harmful Algae*, *48*, 1–11. https://doi.org/10.1016/j.hal.2015.06.008

Nagy, H., Pereiro, D., Yamanaka, T., Cusack, C., Nolan, G., Tinker, J., & Dabrowski, T. (2021). The Irish Atlantic CoCliME case study configuration, validation and application of a downscaled ROMS ocean climate model off SW Ireland. *Harmful Algae*, *107*, 102053. https://doi.org/10.1016/j.hal.2021.102053

Neumann, T. (2010). Climate-change effects on the Baltic Sea ecosystem: A model study. *Journal of Marine Systems*, *81*(3), 213–224. https://doi.org/10.1016/j.jmarsys.2009.12.001

Olbert, A. I., Dabrowski, T., Nash, S., & Hartnett, M. (2012). Regional modelling of the 21st century climate changes in the Irish Sea. *Continental Shelf Research*, *41*(0), 48–60. https://doi.org/10.1016/j.csr.2012.04.003

Pozo Buil, M., Jacox, M. G., Fiechter, J., Alexander, M. A., Bograd, S. J., Curchitser, E. N., et al. (2021). A dynamically downscaled ensemble of future projections for the California current system. *Frontiers in Marine Science*, *8*, 612874. https://doi.org/10.3389/fmars.2021.612874

Praveen, V., Valsala, V., Ajayamohan, R. S., & Balasubramanian, S. (2020). Oceanic mixing over the northern Arabian Sea in a warming scenario: Tug of war between wind and buoyancy forces. *Journal of Physical Oceanography*, *50*(4), 945–964. https://doi.org/10.1175/JPO-D-19-0173.1

Sein, D. V., Groger, M., Cabos, W., Alvarez-Garcia, F. J., Hagemann, S., Pinto, J. G., et al. (2020). Regionally coupled atmosphere-ocean-marine Biogeochemistry model ROM: 2. Studying the climate change signal in the North Atlantic and Europe. *Journal of Advances in Modeling Earth Systems*, *12*(8), e2019MS001646. https://doi.org/10.1029/2019MS001646

Tian, T., Su, J., Boberg, F., Yang, S., & Schmith, T. (2016). Estimating uncertainty caused by ocean heat transport to the North Sea: Experiments downscaling EC-Earth. *Climate Dynamics*, *46*(1–2), 99–110. https://doi.org/10.1007/s00382-015-2571-8

Townhill, B. L., Tinker, J., Jones, M., Pitois, S., Creach, V., Simpson, S. D., et al. (2018). Harmful algal blooms and climate change: Exploring future distribution changes. *ICES Journal of Marine Science*, *75*(6), 1882–1893. https://doi.org/10.1093/icesjms/fsy113

Voldoire, A., Sanchez-Gomez, E., Salas y Melia, D., Decharme, B., Cassou, C., Senesi, S., et al. (2013). The CNRM-CM5.1 global climate model: Description and basic evaluation. *Climate Dynamics*, *40*(9), 2091–2121. https://doi.org/10.1007/s00382-011-1259-y

Watanabe, S., Hajima, T., Sudo, K., Nagashima, T., Takemura, T., Okajima, H., et al. (2011). MIROC-ESM 2010: Model description and basic results of CMIP5-20c3m experiments. *Geoscientific Model Development*, *4*(4), 845–872. https://doi.org/10.5194/gmd-4-845-2011

Wu, T., Song, L., Li, W., Wang, Z., Zhang, H., Xin, X., et al. (2014). An overview of BCC climate system model development and application for climate change studies. *Journal of Meteorological Research*, *28*(1), 34–56. https://doi.org/10.1007/s13351-014-3041-7

Xiu, P., Chai, F., Curchitser, E. N., & Castruccio, F. S. (2018). Future changes in coastal upwelling ecosystems with global warming: The case of the California Current System. *Scientific Reports*, *8*(1), 2866. https://doi.org/10.1038/s41598-018-21247-7

Yu, X., Wang, F., & Tang, X. (2012). Future projection of East China Sea temperature by dynamic downscaling of the IPCC_AR4 CCSM3 model result. *Chinese Journal of Oceanology and Limnology*, *30*(5), 826–842. https://doi.org/10.1007/s00343-012-1290-9